

Adaptation of a gray-box entropy-based model of a gas-driven absorption heat pump for a new low-capacity prototype

Villa, Giorgio¹, Toppi, Tommaso¹, Aprile, Marcello¹, Motta, Mario¹

¹ Department of Energy, Politecnico di Milano, 20156 Milan, Italy

E-mail address: giorgio.villa@polimi.it (G. Villa)

Abstract:

In this work, a gray-box model of a gas driven absorption heat pump previously used to describe the performances of a 40kW commercial unit is adapted to characterize the steady-state behavior of a new low-capacity gas driven heat pump prototype. The results show that the model is still very accurate, although the two heat pumps differ in terms of capacity and thermodynamic cycle. After modifying a few parameters, the deviation between the performances calculated by the model and the experimental ones are lower than 3%.

1 Introduction

The physical phenomena that take place in absorption heat pumps are difficult to describe with a mathematical model. In fact, an existing model that sets conservation equations on each component provides a system of non-linear equation to solve [1]. However, to perform year-round energy simulation of the building system, simplified models easier to solve are convenient. For this reason, several empirical and semi-empirical models of absorption heat pumps have been developed. A comparison of different models is shown in [2]. It concludes that the models shown in [3] and in [4] can be used to obtain relative errors between the calculated quantities and the experimental ones lower than 10%. The first one [3] calculates the COP as function of the Carnot efficiency and a set of parameters to identify experimentally. The second one [4] calculates the thermal power as a linear function dependent on ΔT that is the so called characteristic temperature function. An additional very accurate model is shown in [5]. The gas-driven absorption heat pump (GHP) model consists in a gray-box model of the combustion chamber, a lumped parameter model of the flue gas heat exchanger and an entropy-based model of the ammonia-water GAX cycle. It was calibrated on a 40kW commercial unit with a gas burner nominal capacity of 28.2 kW. In this work, this model is calibrated on experimental data provided by an air-water gas driven heat pump prototype with a nominal capacity of the gas burner of 6.69 kW. In addition, the original model is based on a commercial unit designed with a different heat generator technology and a slightly different thermodynamic cycle with respect to the prototype. To do that, the model has been slightly modified with an additional parameter to identify, in order to obtain a more general model. The main goal of this work is to evaluate the accuracy of the entropy-based model also for low capacity GHP. In the following chapters, a brief presentation of the original gray-box model and the difficulties met to calibrate the model on a different GHP are described. To conclude, the results obtained by the recalibration process are shown.

2 Gray-box model description

2.1 General description of the model

The original model [5] divides the GHP in three main parts, as shown in Figure 1:

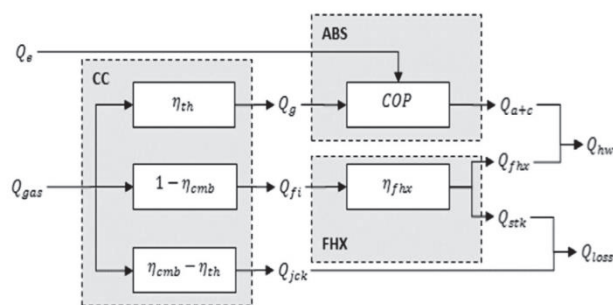


Figure 1: GHP thermodynamic cycle

- Combustion chamber (CC): in this component and in the generator, a complex mass transfer and a radiative-convective heat transfer take place. Thus, a simple integral model of the gas furnace and generator calculates the heat input to the generator (Q_g), the mass flow rate on dry gas basis ($\dot{m}_{f,dry}$), and the temperature of the gases leaving the chamber (T_{fi}). The inputs are the gas input (Q_{gas}), the combustion efficiency (η_{cmb}) and the thermal efficiency (η_{th}). The efficiencies are assumed constant and equal to 0.82 and 0.80 respectively [5].

- Flue gas heat exchanger (FHX): The model is based on the approach used for condensing coils [6]. It calculates the heat recovered from flue gases (Q_{fhx}) to heat up the inlet water. The inputs are $\dot{m}_{f,dry}$ and T_{fi} , calculated by

the combustion chamber model, and the heat exchanger UA-value in condensation (UA_{wet}) that is identified with experimental data.

- Absorption cycle (ABS): The qualitative representation of the absorption cycle is shown in Figure 2. The diagram is specific to the heat input (Q_g), provided by the combustion of the natural gas. In fact, α is defined as the ratio between the heat leaving the absorber (Q_a) and the input heat at the generator (Q_g). Then, the heat input at the evaporator divided by the heat input at the generator is (COP-1), thus the energy balance of the system, neglecting the work input at the solution pump and the heat losses, gives the heat leaving the condenser (COP- α).

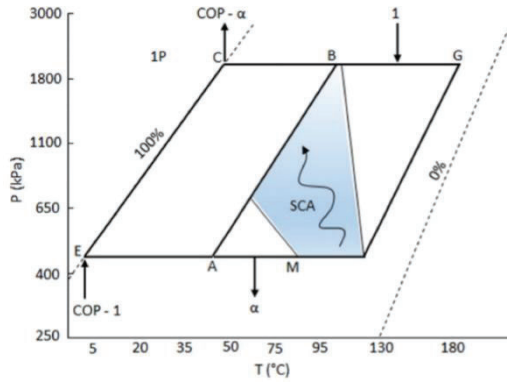


Figure 2: Absorption cycle in a P - T - x diagram – (A) rich solution leaving the absorber, (B) bubble point generator feed, (G) poor solution at the base of the generator, (M) mixing point between refrigerant vapor and solution leaving the Solution cooler absorber (SCA)

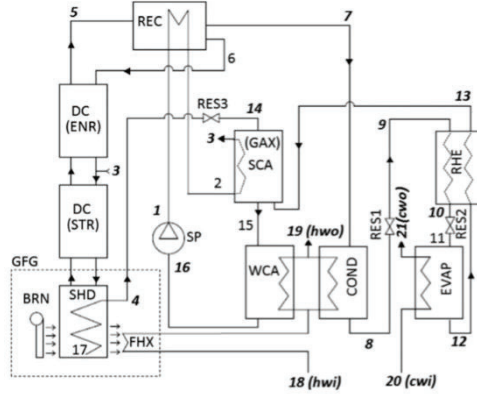


Figure 3: GHP scheme - gas burner (BRN), solution heated desorber (SHD), flue gas heat exchanger (FHX), distillation column (DC), rectifier (REC), solution cooled absorber (SCA), water cooler absorber (WCA), condenser (COND), evaporator (EVAP), refrigerant heat exchanger (RHE), restrictor (RES)

2.2 How the model works

The model is based on the entropy balance shown in (1). The goal is to calculate the outputs of the GHP using as input the inlet water mass flow rate (\dot{m}_{hw}) and temperature (T_{hwi}), the inlet brine mass flow rate (\dot{m}_{cw}) and temperature (T_{cwi}), and the heat input (Q_g).

$$\Delta S_{IRR} + \frac{Q_g}{T_g} + \frac{Q_E}{T_E} = \frac{Q_a}{T_a} + \frac{Q_C}{T_C} \quad (1)$$

Writing the balance per unit of heat input at the generator and solving for COP, the equation (2) is obtained. COP is defined as the ratio between the heat output of the absorption cycle ($Q_a + Q_C$) and the heat input (Q_g). δ_{INT} is the ratio between ΔS_{IRR} and the heat input at the generator (Q_g).

$$COP = \frac{T_C T_g - T_E}{T_g T_C - T_E} + \alpha \frac{T_E T_C - T_a}{T_a T_C - T_E} - \delta_{INT} \frac{T_E T_C}{T_C - T_E} \quad (2)$$

Being an entropy-based model, the computation of the internal entropic average temperature is needed. The heat input provided by the natural gas combustion occurs at an intermediate temperature (T_g) between (B) and (G), while the Q_a heat output occurs at (T_a), between (A) and (M). It is assumed, on experimental basis, that the heat leaving the condenser (Q_C) occurs at temperature (T_C) that is equal to the water leaving the condenser (T_{hwo}). The temperature (T_E), correspondent to the heat input at the evaporator (Q_E), should be calculated considering the refrigerant mass fraction (x_r) and the pressure (P_{low}). However, temperatures and pressure are unknown, thus an iterative process that involves several pre-set parameters takes place. First, the output water temperatures of the condenser (T_{hwo}) and the evaporator (T_{cwo}) are calculated as in (3) and (4), showing the need for an iterative solver. Then, the temperatures of the absorption cycle T_E and T_a are calculated as in (5) and (6). Experiments show that T_E can be assumed close to T_{cwo} [7]. However, below a critical value of the temperature difference $T_{hwi} - T_{cwo}$, the difference between T_E and T_{cwo} changes rapidly. For this reason, a piecewise linear interpolant has been used, as shown by equation (5). $c_{p,hw}$ and $c_{p,cw}$ are assumed constant and equal to 4.186 kJ K⁻¹kg⁻¹ and 3.6 kJ K⁻¹kg⁻¹ respectively.

$$T_{cwo} = T_{cwi} - \frac{(COP - 1)Q_g}{\dot{m}_{cw}c_{p,cw}} \quad (3)$$

$$T_{hwo} = T_{hwi} + \frac{COP Q_g + Q_{fhx}}{\dot{m}_{hw}c_{p,hw}} \quad (4)$$

$$T_E = \begin{cases} T_{cwo} - e_1 - e_2 (T_{hwi} - T_{cwo}) & (T_{hwi} - T_{cwo}) < e_0 \\ T_{cwo} - e_1 - e_0 (e_2 - e_3) - e_3 (T_{hwi} - T_{cwo}) & (T_{hwi} - T_{cwo}) \geq e_0 \end{cases} \quad (5)$$

$$T_A = T_{hwi} + a_0 \quad (6)$$

Assuming the ammonia concentration (x_r) constant and equal to 0.98 [5], the pressure P_{low} and P_{high} can be calculated as bubble point pressures at T_E and T_C respectively. Then, x_A is calculated as the equilibrium mass fraction of the liquid phase at T_A and P_A , which is equal to P_{low} minus the pressure drop through the absorber (20 kPa) [5]. At this point, T_B is calculated as the bubble point temperature at P_{high} and x_A . To conclude, T_M , T_G , and δ_{INT} are calculated as in (7), (8) and (9). Solving the system with the secant method, letting varying COP within 1 and 2, the outputs of the thermodynamic cycle can be calculated. To conclude, the Gas Utilization Efficiency (GUE) is calculated as in (10).

$$T_M = m_0 + m_1 T_E + m_2 T_A + m_3 T_B \quad (7)$$

$$T_G = g_0 + g_1 T_E + g_2 T_A + g_3 T_B \quad (8)$$

$$\delta_{INT} = (s_0 + s_1 T_A + s_2 T_B) \left(1 + \left| f_1 (T_B - T_A) + f_2 * \frac{Q_g}{Q_{g,nom}} \right|^+ \right) \quad (9)$$

$$GUE = \frac{Q_a + Q_c + Q_{fhx}}{Q_{gas}} \quad (10)$$

2.3 Parameters identification

The model uses several parameters that have to be defined (UA_{wet} , e_0 , e_1 , e_2 , e_3 , m_0 , m_1 , m_2 , m_3 , g_0 , g_1 , g_2 , g_3 , s_0 , s_1 , s_2 , f_1 , f_2 , a_0 , α). a_0 and α are predefined parameters equal to 7°C and 0.95 respectively, in accordance with experimental data [7]. The other parameters are set using the following identification procedures. All the parameters, except for f_1 and f_2 , are identified using seven experimental test measurements at nominal gas input and constant ΔT_{hw} and ΔT_{cw} . f_1 and f_2 are identified using two additional tests at partial loads.

- UA_{wet} is calculated by means of an identification process, which minimises the root mean square error (RMSE) of the energy balance (11), where the heat pump useful effect (\tilde{Q}_{hw}), the natural gas input (\tilde{Q}_{gas}), and the heat exchanged at the evaporator (\tilde{Q}_e) are experimental values. The only unknown is the heat recovered by the flue gas heat exchanger (Q_{fhx}), which depends on UA_{wet} as in the model in [6].

$$\tilde{Q}_e = (\tilde{Q}_{hw} - Q_{fhx}) - \eta_{th} \tilde{Q}_{gas} \quad (11)$$

- e_0 , e_1 , e_2 , e_3 are calculated minimizing the RMSE between the T_E , calculated with the equation (5) and the T_E indirectly measured using the refrigerant concentration (x_r) and the experimental value of P_{low} .

- m_0 , m_1 , m_2 , m_3 are calculated minimizing the RMSE between T_M calculated by the equation (7) and T_M calculated using the energy balance of the absorber, as shown by the equation (12). T_A is calculated by equation (6), while \dot{m}_{ps} and \dot{m}_r are calculated by equation (13) and (14). $c_{p,sol}$ is the average equivalent specific heat of the two-phase mixture. It is assumed constant and equal to 17 kJ K⁻¹kg⁻¹ for the typical range of concentrations, pressures and qualities at the inlet of the absorber [5]. Δh_e is the enthalpy increase of the refrigerant in the evaporator that can be considered nearly constant and equal to 1050 kJ kg⁻¹ [5]. ρ_B is the density evaluated at T_B .

$$\alpha Q_g = (\dot{m}_{ps} + \dot{m}_r) c_{p,sol} (T_M - T_A) \quad (12)$$

$$\dot{m}_{ps} = k \sqrt{\rho_B (P_{high} - P_{low})} \quad (13)$$

$$\dot{m}_r = \frac{Q_g (COP - 1)}{\Delta h_e} \quad (14)$$

- g_0 , g_1 , g_2 , g_3 are calculated minimizing the RMSE between the T_G calculated by equation (8) and the T_G calculated as the bubble point temperature at P_{high} and x_G . The latter is obtained from the mass and species balance equation of the desorber system, as shown by equation (15).

$$x_G = x_A - (x_r - x_A) \frac{\dot{m}_r}{\dot{m}_{ps}} \quad (15)$$

- s_0 , s_1 , s_2 , f_1 , f_2 are calculated minimizing the RMSE between the COP calculated by equation (2) and the COP calculated with the experimental data.

The original model is based on a water-water commercial heat pump with a nominal capacity of the generator of 28.2 kW. In this work, the same model is used to calculate the performances of an air-water GHP prototype with a nominal heat capacity of the generator of 6.69 kW. Despite they use different heat sources (air and water) they are comparable because the prototype has a secondary loop that heats up the brine flow with outdoor air. Therefore,

to complete the model of the air-water heat pump, the air-water heat exchanger has to be added (not considered in this paper). Moreover, the absorption cycle and the generator of the prototype are slightly different from the ones showed in figure 3. In fact, the prototype has an additional solution heat exchanger between the SCA and the SHD. Then, the commercial heat pump has a cross-tube generator, while the prototype has a fire-tube generator, which has the advantage of lower heat losses and better heat distribution. To perform the identification phase, a set of experimental data similar to the one used in [5] was measured. Moreover, two small changes among the predefined parameters, defined in the previous chapters (x_r , $c_{p,sol}$, Δh_e etc.), have been done. $Q_{gas,n}$ is 6.69 kW instead of 28.8 kW. Then, the value of k , used by equation (13), in the original model [5] was set having a deep knowledge of the restrictor RES3, shown in figure 3. However, the restrictor used in the 40 kW commercial unit is quite different from the restrictor used by the prototype. To solve this issue, two ways are available:

- Simplified k method: It is assumed that the k varies linearly with $Q_{gas,n}$. For the prototype, it is equal to 0.154.
- Advanced k method: An additional parameter (k_k) is defined and the new value of k is calculated dividing the k obtained with the simplified method by the additional parameter k_k . To define the value of k_k a minimization process of the RMSE between the experimental GUE and the GUE calculated by the model is performed, obtaining a value of k_k equal to 1.64.

Table 1 – Identified parameters for the prototype, simplified method (value1) and advanced method (value 2)

Parameter	Value 1	Value 2	Unit	Parameter	Value 1	Value 2	Unit
UA_{wet}	3.374E-3	3.600E-3	$kg\ s^{-1}$	g_0	201.595	423.996	$^{\circ}C$
e_0	32.405	32.575	$^{\circ}C$	g_1	0.999	3.872	-
e_1	22.501	24.187	$^{\circ}C$	g_2	-1.707	-6.732	-
e_2	-0.572	-0.638	-	g_3	0.623	1.299	-
e_3	0.035	0.032	-	s_0	2.099E-4	7.715E-4	K^{-1}
m_0	35.186	29.666	$^{\circ}C$	s_1	7.725E-6	-8.109E-6	K^{-2}
m_1	-0.858	-1.202	-	s_2	3.946E-6	7.541E-9	K^{-2}
m_2	1.743	2.015	-	f_1	0.023	0.016	K^{-1}
m_3	-0.290	-0.231	-	f_2	-2.163	-1.589	-

3 Results

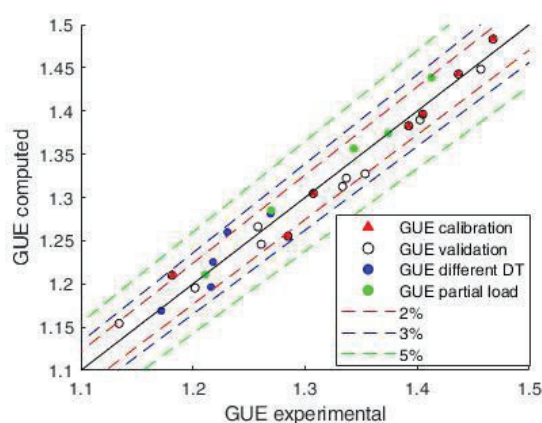
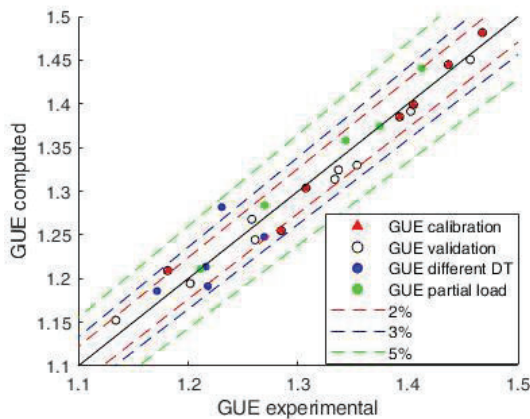


Figure 4 – Model accuracy, simplified method ($k_k=1$) Figure 5 – Model accuracy, advanced method ($k_k=1.64$)

Figure 4 and figure 5 show the comparison between the GUEs calculated by the model in different conditions and the experimental GUEs in the same conditions. Figure 4 shows the results obtained using the simplified approach, while figure 5 shows the results obtained using the advanced method to define k . In both cases, several working conditions are taken into account, such as different inlet water temperatures (T_{hwi}), different outlet temperature set points (T_{hwo}), partial load, and different inlet temperatures at the evaporator (T_{cwi}).

4 Conclusions

The results show that the proposed model describes accurately the performances of the prototype, although it has a different generator, thermodynamic cycle and nominal capacity with respect to the commercial unit. The difference between the GUEs calculated by the model and the experimental ones are always lower than 3%, except for one case. Furthermore, using the advanced method, the accuracy of the model increases reaching a deviation between the experimental values and the calculated ones, usually lower than 2%.

5 List of References

- [1] G. Grossman and A. Zaltash, "ABSIM-modular simulation of advanced absorption systems," *International Journal of Refrigeration*, vol. 24, pp. 531-543, 2001.
- [2] F. Boudéhenn, S. Bonnot, H. Demasles and A. Lazrak, "Comparison of different modeling methods for a single effect water-lithium bromide absorption chiller," in *Proceeding of EuroSun 2014*, Aix-les-Bains, France, 2014.
- [3] A. Le Denn, F. Boudehenn, D. Mugnier and P. Papillon, "A simple predesign tool for solar cooling, heating and domestic hot water production systems," *Proceedings 13th Conference of International Building Performance Simulation Association*, pp. 1031-1036, 2013.
- [4] A. Kühn and F. Ziegler, "Operational results of a 10kWabsorption chiller and adaptation of the characteristic equation," in *Proceeding of First International Conference on Solar Air Conditioning*, Bad-Saffelstein, Germany, 2005.
- [5] M. Aprile, R. Scoccia, T. Toppi and M. Motta, "Gray-box entropy-based model of a water-source NH₃-H₂O gas-driven absorption heat pump," *Applied Thermal Engineering*, vol. 118, pp. 214-223, 2017.
- [6] J. L. Threlkeld, *Thermal Environmental Engineering*, New York: Pretice-Hall, 1970.
- [7] M. Aprile, R. Scoccia, T. Toppi, M. Guerra and M. Motta, "Modelling and experimental analysis of a GAX NH₃-H₂O gas-driven absorption heat pump," *International Journal of refrigeration*, vol. 66, pp. 145-155, 2016.